

Cite this: *Nanoscale Adv.*, 2020, 2,
3942Received 5th April 2020
Accepted 22nd July 2020

DOI: 10.1039/d0na00271b

rsc.li/nanoscale-advances

Platelet mediated TRAIL delivery for efficiently targeting circulating tumor cells†

Nerymar Ortiz-Otero,^a Jocelyn R. Marshall,^a Bradley W. Lash^b
and Michael R. King^{ib}*^c

Several studies have demonstrated the role of platelets in promoting cancer metastasis. Platelets bind to and protect circulating tumor cells (CTCs) from hemodynamic forces and immune cells, and also promote tumor cell arrest in the vasculature and extravasation. Thus, platelets represent a promising vehicle to deliver anticancer therapeutic agents to CTCs. In this study, we developed a novel platelet-mediated TNF-related apoptosis inducing ligand (TRAIL) delivery system to target CTCs and hinder metastasis *via* “*in situ*” platelet modification. This platelet-mediated TRAIL delivery significantly reduced the viability of colorectal and breast cancer cells circulating in flowing blood under physiological shear conditions. TRAIL-coated platelets significantly killed over 60% of CTCs in flowing blood from a variety of primary metastatic cancer samples. Platelets have been considered an important player in the regulation of metastasis due to their interaction with cancer cells in the circulation; the current study supports the idea of using platelet-based TRAIL delivery as a promising CTC-targeted cancer therapy.

Introduction

Metastasis refers to the spread of cancer cells from the primary tumor to distant organs, and is responsible for 90% of cancer-related deaths.¹ Cancer patients diagnosed with metastatic cancer disease have poor probability of survival due to the fact that there are no currently available therapies targeting metastasis.² In spite of the high mortality attributed to metastasis, it is considered an inefficient process due to the fact that only 0.01% of tumor cells can successfully grow in distant organs.^{3,4} Tumor cells migrate along with other stromal cells including platelets, to enhance their survival and migration.^{5,6}

Platelets are anucleated cells and their main function is to maintain hemostasis and vascular integrity.⁷ For many decades, the pro-metastatic function of platelets has been well documented, with platelets playing a role in tumor mass expansion, tumor cell migration and growth in distant organs.⁸ One of the most important functions of platelets is that they adhere to CTCs and create a cellular shield which protects CTCs from hemodynamic force and cytotoxic effects of immune cells.^{9–12} This platelet-tumor cell interaction further enhances tumor cell arrest in the vasculature and eventually results in metastasis.¹²

As a key regulator of the metastatic process, platelets represent a potential target as well as an efficient vehicle to deliver novel cancer therapeutic agents. Various antithrombotic agents have been examined for their efficacy in reducing thrombotic events and the metastatic burden in cancer patients. Clinical studies demonstrate the benefits of anticoagulants in treating patients with local disease over patients with systemic disease.^{13,14} However, using anticoagulants as a long-term cancer therapy is associated with higher risk due to excessive bleeding. Since then, efforts have been made to develop anti-cancer therapies by targeting platelets or coagulation pathway regulators, without affecting hemostasis.

Recent studies demonstrate a potential strategy for delivering cancer therapeutic agents to CTCs, based on the creation of artificial “platelet-like” particles. Several studies have successfully packaged cytotoxic agents such as doxorubicin in human platelet membranes or platelet-mimicking nanoparticles. These platelet-like particles reduce the metastatic burden in *in vivo* mouse models.^{15–17} Moreover, recent studies suggest that functionalizing platelet membranes with cytotoxic drugs is more efficient in killing CTCs and reducing cancer metastasis than loading the cytotoxic drug into the platelets.^{18–20} While coagulation is understood to be generally pro-metastatic, in these platelet-based delivery approaches care is usually taken to ensure that normal hemostatic function is not disrupted.^{18,19} On the contrary, some researchers have developed therapeutic approaches that disrupt platelet-tumor cell interactions to reduce the formation of macro-metastases.^{21,22} All the above-mentioned approaches present effective anti-cancer strategies both *in vitro* and *in vivo*, however these are not cost-effective for

^aMeinig School of Biomedical Engineering, Cornell University, Ithaca, NY 14850, USA.
E-mail: mike.king@vanderbilt.edu

^bLehigh Valley Health Network, Allentown, PA 18103, USA

^cDepartment of Biomedical Engineering, Vanderbilt University, Nashville, TN 37202, USA

† Electronic supplementary information (ESI) available. See DOI: 10.1039/d0na00271b



clinical applications due to the *ex vivo* modification of platelets. Thus, further studies are needed to improve the delivery of platelet-based cancer therapy for clinical purposes.

In this study, we developed a novel platelet-based TRAIL delivery system that allows us to modify the platelet “*in situ*” to deliver a therapeutic agent to CTCs. This novel approach

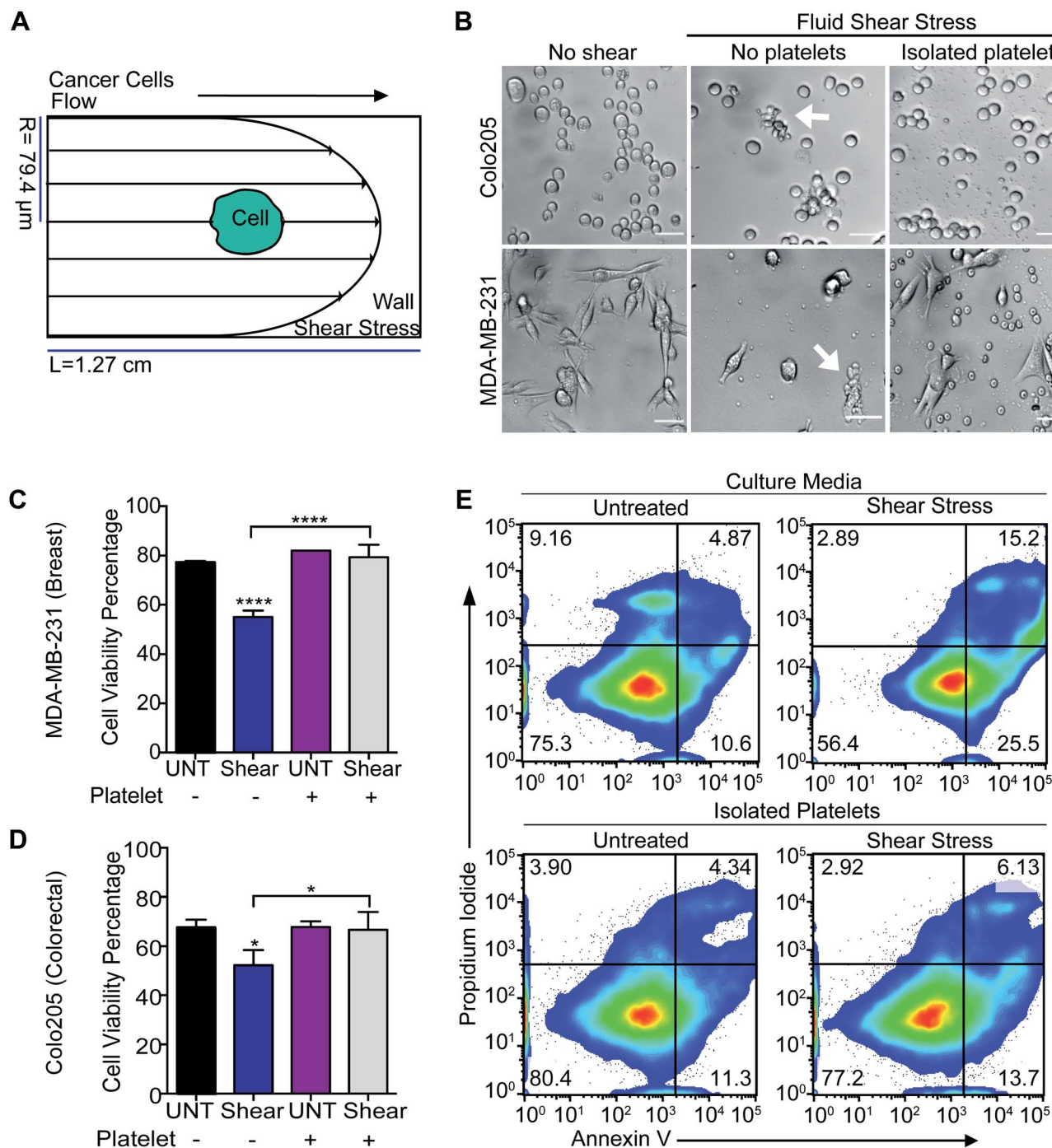


Fig. 1 Platelet adhesion to tumor cells enhances their survival in FSS. (A) Diagram of the fluid shear stress that the tumor cells experience. (B) Bright-field images of breast and colorectal cancer cells subjected to FSS with and without incubation with isolated human platelets. Scale bar is $40 \mu\text{m}$. White arrows are showing dead cells. (C) Bar graph represents the viability percentage of breast cancer cells exposed to FSS before and after being incubated with isolated platelets (mean \pm SD, $N = 3$). Significance (**** $P < 0.0001$) in cell viability reduction was calculated using a one-way ANOVA test. (D) Bar graph represents the viability percentage of colorectal cancer cells exposed to FSS before and after being incubated with isolated human platelets (mean \pm SD, $N = 3$). An insignificant reduction (* $P < 0.258$) of cell viability was determined using a one-way ANOVA test. (E) Flow cytometry density plots display the viability of breast cancer cells after being exposed to FSS with and without co-incubation with isolated human platelets. The viability assay divides the chart into four quadrants, which represent the sub-populations of cells undergoing apoptosis (lower left: viable cells, lower right: early apoptotic cells, upper right: late apoptotic cells, upper left: necrotic cells).



consists of nanoscale liposomes decorated with TRAIL, a protein that selectively induces apoptosis in tumor cells while sparing normal cells and von Willebrand Factor A₁ domain

(vWFA₁), a protein that is able to bind to the platelet receptor complex GPIb-IX-V.²³ Here, we hypothesize that coating platelets with TRAIL *via* the vWFA₁ domain will induce apoptosis of

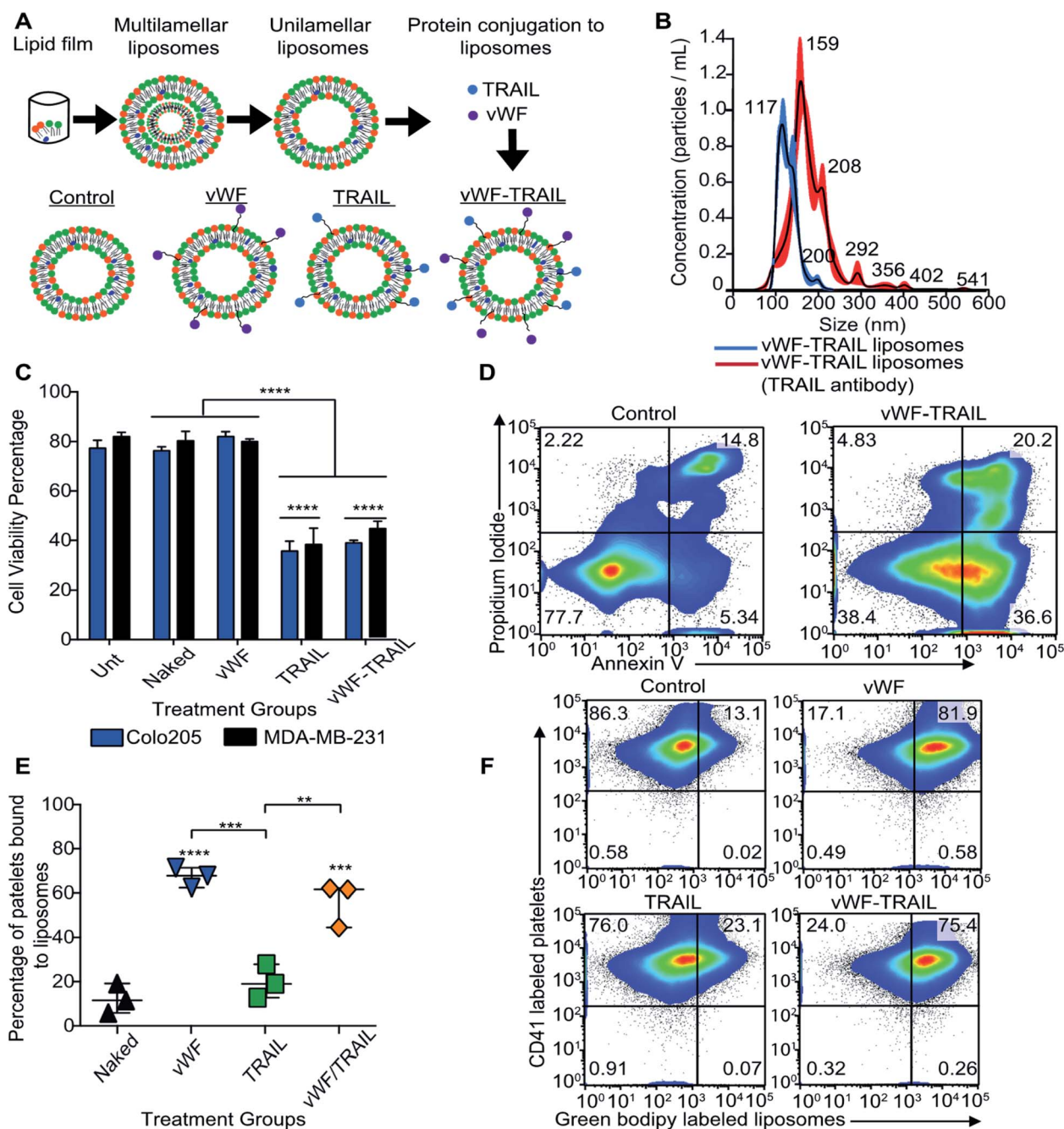


Fig. 2 Planned modification *in situ* of human platelets to display TRAIL on their surface *via* vWF interactions. (A) Diagram shows the preparation of nanoscale liposomes using a thin film method. Four groups were used in the study, including: Naked control, vWF, TRAIL, and vWF-TRAIL liposomes. (B) The size distribution of the vWF-TRAIL liposome group before and after antibody conjugation with anti-CD253 (TRAIL). The shift in size distribution represents the fraction of particles containing TRAIL on the particle surface. (C) Bar graph represents the viability percentage of Colo205 and MDA-MB-231 treated with the four different liposome formulations under static conditions with untreated controls (mean \pm SD, $N = 3$). A significant reduction (**** $P < 0.0001$) of cellular viability was determined using a two-way ANOVA test (two conditions: treatment and type of cancer). (D) Flow cytometry density plots represent the viability of MDA-MB-231 cancer cells after being treated with control and vWF-TRAIL liposomes under static conditions. (E) Scatter dot plot shows the percentage of platelets that had bound functionalized liposomes in flowing blood after 30 min (mean \pm SD, $N = 3$). Significant increase (**** $P < 0.0001$, *** $P < 0.0004$ and ** $P = 0.0016$) in adhesion of vWF-functionalized liposomes to platelets compared with the control liposomes was determined using a one-way ANOVA test. (F) Flow cytometry plots show the percentage of platelets that had bound functionalized liposomes (upper right quadrant).



CTCs and eliminate them from circulation. Our study demonstrates that TRAIL-coated platelets efficiently target and kill CTCs under conditions of shear stress using an *ex vivo* CTC model. Two different shear stress ranges are studied. In the first section with cancer cell lines, short, extremely high pulses of fluid shear are introduced, to determine the factors that promote shear damage and survival of cancer cells; while in the second part, sustained exposure to venous shear flow was used to test the efficacy of our experimental therapeutic.

Results and discussion

Platelet adhesion enhances the survival of metastatic tumor cells under high fluid shear stress

To determine whether platelets hold the potential to deliver TRAIL to tumor cells in the circulation, the adhesion of platelets to tumor cells was evaluated under high fluid shear stress (FSS) along with the effect on cancer cell viability (Fig. 1A). Colorectal and breast cancer cells were subjected to high magnitude of FSS (~ 5920 dyn cm^{-2}).²³ This level of shear stress represents regions of the vasculature such as arterial bifurcations and jetting heart valves, and is typically experienced by blood over brief periods of under 1 s.²⁴ We observed that high FSS reduced the viability of breast and colorectal cancer cells, by 25% and 20%, respectively. Importantly, cancer cells pre-incubated with isolated human platelets had a higher viability percentage, similar to untreated control samples (Fig. 1B–E). Platelets may have adhered to the cancer cells to form a protective shield that could protect the cancer cells under high FSS, although this deserves further study.

TRAIL delivery to tumor cells *via* platelets

Our next question was whether platelets can be modified *in situ* for functional TRAIL delivery to tumor cells in the bloodstream. To address this question, a formulation of liposomes was prepared to integrate TRAIL onto the platelet *via* vWF_{A1} interactions. The liposomes were conjugated with vWF-A₁ and TRAIL on their surface (Fig. 2A). Four liposomal groups were used throughout the study: Control, vWF, TRAIL, and vWF-TRAIL. Previously, we showed that soluble TRAIL has negligible activity at these concentrations.²⁵ To confirm the successful conjugation of vWF-A₁ and TRAIL protein on the liposome surface, liposomes were characterized for their size, surface charge, polydispersity index (PDI), particle concentration and percentage of TRAIL-coated particles. The vWF-TRAIL liposomes were 136 ± 1.2 nm in size, with a surface charge of 0.10 ± 0.01 , PDI 0.122 ± 0.05 , and a concentration of 4.45×10^{10}

particles per mL. The values for different liposomal formulations are given in Table 1. As these parameters do not conclusively confirm protein conjugation on the surface, further experiments were performed to evaluate the presence of TRAIL in the liposomal formulations. Liposomes were incubated with TRAIL antibody overnight and the change in size was evaluated using a NanoSight NS300 instrument. It was determined that 90% of the liposome particles contained at least one TRAIL molecule attached to the particle surface based on the shift in the size distribution curve (Fig. 2B). We further investigated the functional efficacy of our formulations in inducing apoptosis in cancer cells and binding to human platelets in flowing blood. It was found that 20 μL of vWF-TRAIL liposomes reduced cell viability of colorectal and breast cancer cells by 40% under static conditions (Fig. 2C and D). In addition, under physiological shear conditions (225 s^{-1}) we observed a ~ 6 -fold increase in the percentage of platelets attached to vWF and vWF-TRAIL conjugated liposomes compared to control and TRAIL liposome groups (Fig. 2E and F). Collectively, these results demonstrate successful preparation of functionalized liposomes, with vWF-TRAIL liposomes efficiently delivering TRAIL and targeting CTCs.

In situ TRAIL delivery under physiological conditions kills colorectal and breast cancer cells

We next investigated whether the targeted delivery of TRAIL *via* platelets could kill tumor cells in flowing blood. Colorectal and breast cancer cells were spiked into whole blood and treated with the functionalized liposomes for 2 h under physiological shear conditions in a cone-and-plate viscometer. It was found that vWF-TRAIL liposomes dramatically reduced the viability of Colo205 and MDA-MB-231 cancer cells by 60% and 70%, respectively, compared to control liposomes (Fig. 3A–C). Importantly, vWF-TRAIL liposomes eliminated cancer cells up to threefold compared to samples treated with the control and vWF liposomes (Fig. 3D). Moreover, this approach did not affect the platelet-tumor cell interaction in the blood (ESI Fig. 1S, A and B†). Overall, these results indicate that vWF-TRAIL liposomes adhere to human platelets under shear conditions to create TRAIL-coated platelets and efficiently kill aggressive colorectal and breast cancer cells in blood *ex vivo*.

TRAIL conjugation and functionalization of platelets does not induce platelet activation

We assessed whether liposome-mediated delivery of TRAIL *via* platelets affects the physiological function of the platelets. To

Table 1 Characterization of the functionalized liposomes *via* measurement of several parameters: diameter, polydispersity index (PDI), zeta potential and nanoparticle concentration

| Sample | Diameter (nm) | PDI value | Zeta potential (mV) | Concentration (particles $\times 10^{10} \text{ mL}^{-1}$) |
|-----------|-------------------|-----------------|---------------------|---|
| Control | 134.70 ± 1.47 | 0.17 ± 0.03 | -5.00 ± 0.39 | 4.85 ± 0.07 |
| vWF | 139.20 ± 1.47 | 0.26 ± 0.06 | -3.70 ± 0.29 | 4.39 ± 0.12 |
| TRAIL | 136.70 ± 1.07 | 0.12 ± 0.05 | -0.02 ± 0.01 | 4.64 ± 0.09 |
| vWF-TRAIL | 135.97 ± 1.13 | 0.12 ± 0.05 | 0.10 ± 0.01 | 4.45 ± 0.10 |



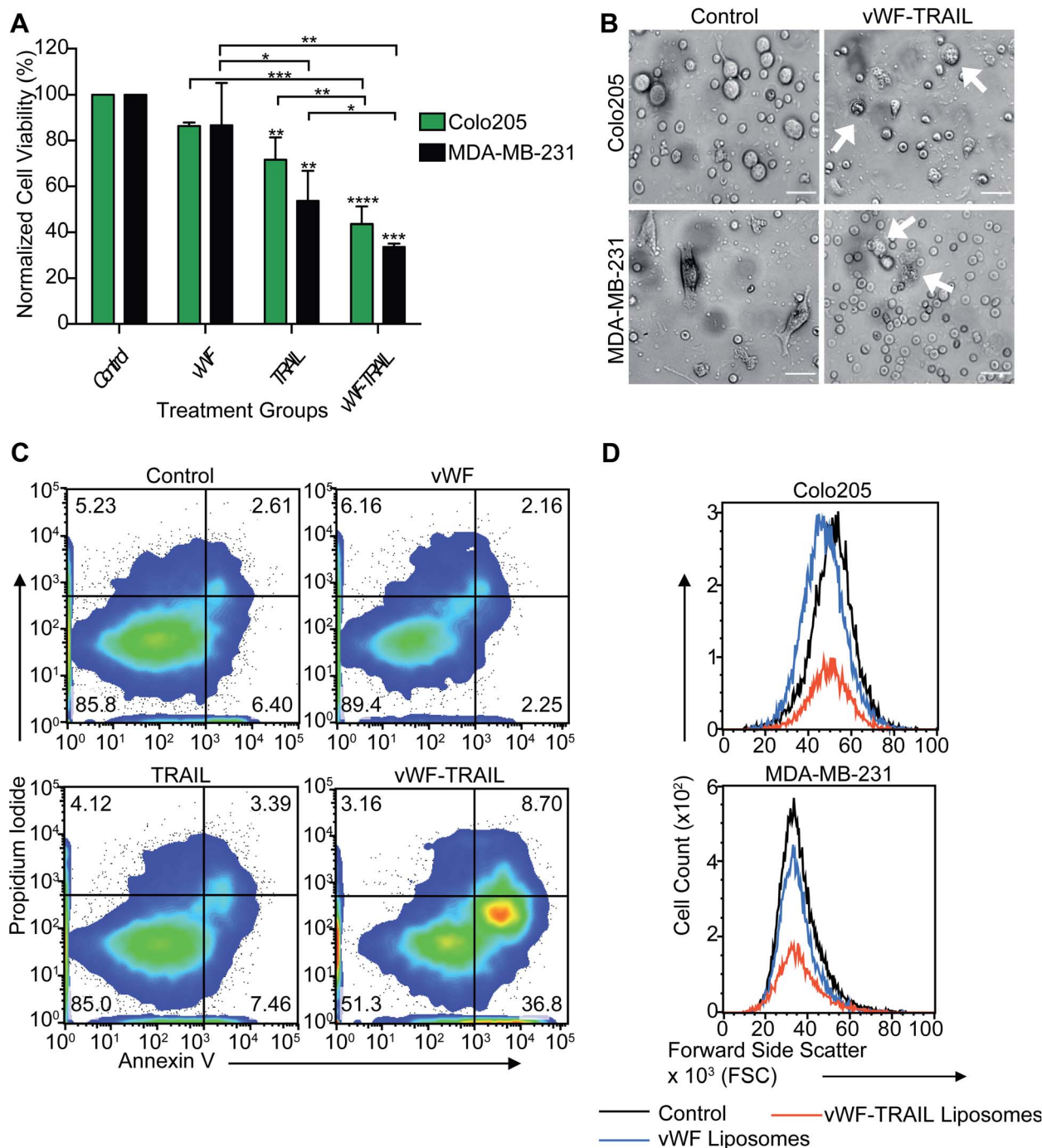


Fig. 3 TRAIL-coated platelets kill breast and colorectal cancer cells in flowing blood. (A) Bar graph shows the viability percentage of Colo205 and MDA-MB-231 cancer cells treated with functionalized liposomes in flowing blood for 2 h (mean \pm SD, $N = 3$). Significance in the cell viability percentage (**** $P < 0.0001$, *** $P < 0.0007$, ** $P < 0.0094$ and * $P = 0.04277$) was testing using two-way ANOVA test (two conditions: treatment and type of cancer). (B) Bright-field images of breast and colorectal cancer cells treated with functionalized liposomes in flowing blood. White arrows indicate dead cells. Scalebar is 40 μm . (C) Flow cytometry density plots show viable breast cancer cells undergoing apoptosis after being treated with functionalized vWF-TRAIL liposomes. (D) Flow cytometry histograms represent the viable cell counts of breast and colorectal cancer cells after being treated with naked control, vWF and vWF-TRAIL liposomes.

detect any side effects of TRAIL liposome interaction with platelets, we incubated isolated platelets with functionalized liposomes and measured the degree of platelet activation corresponding different stages in hemostatic function: (i) intracellular levels of calcium, (ii) activation of integrins, (iii)

secretion of platelet microparticles and (iv) expression of P-selectin on the platelet surface (expected to increase in activated platelets). No increase in intracellular calcium was detected when the platelets were incubated with functionalized liposomes compared to thrombin-treated platelets (Fig. 4A and



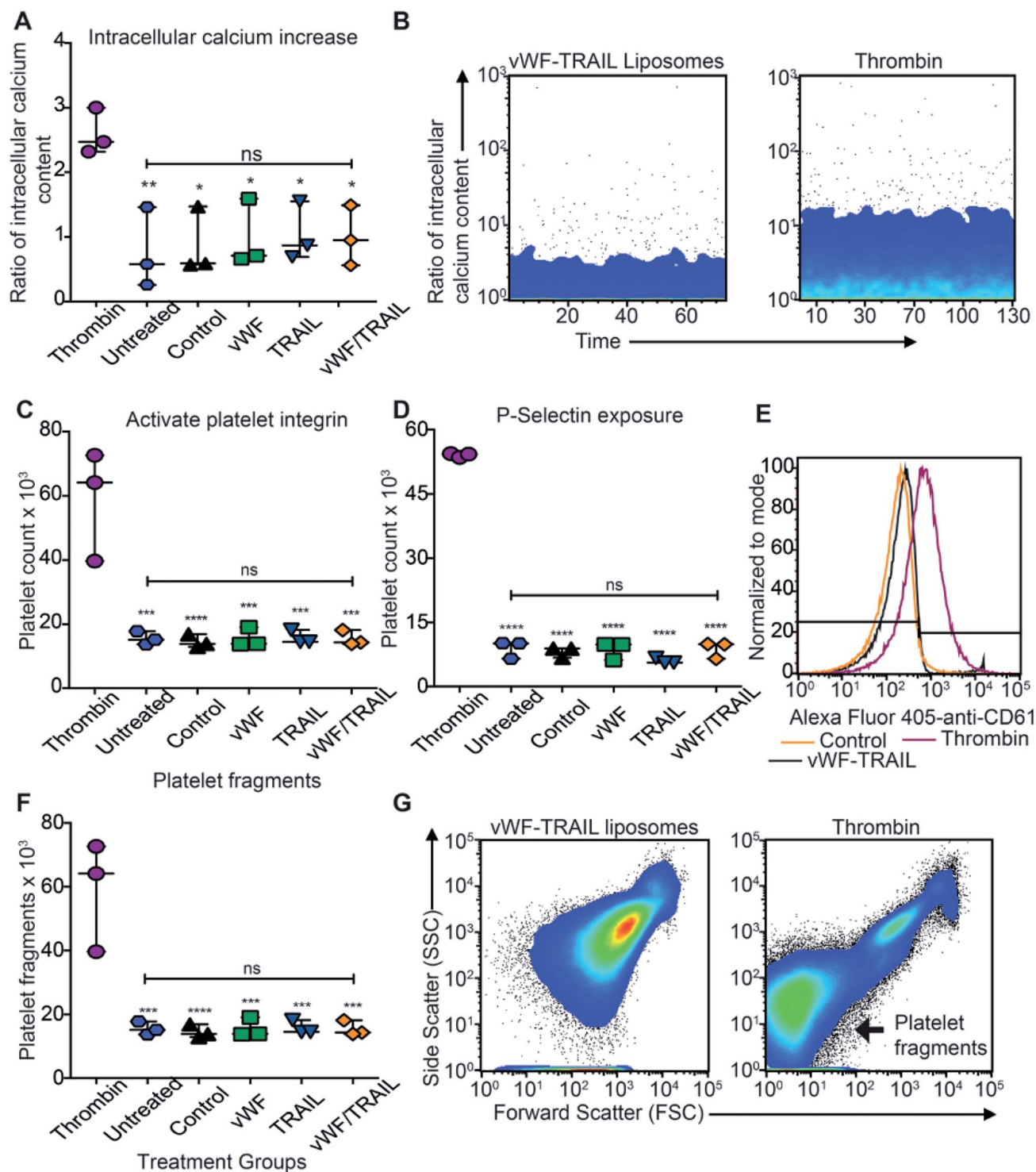


Fig. 4 TRAIL delivery via platelets does not induce platelet activation. (A) Scatter dot plot displays the intracellular content of calcium in isolated human platelets after being treated with the functionalized liposomes (mean \pm SD, $N = 3$). Significance of the increase of intracellular content versus thrombin control (** $P = 0.0071$ and * $P < 0.0217$) was calculated using one-way ANOVA test. (B) Flow cytometry charts show the intracellular calcium content over time in isolated platelets treated with vWF-TRAIL liposomes and thrombin at a concentration of 1 U mL^{-1} . (C) Scatter dot plot represents the number of platelets displaying the activated form of $\alpha_{IIb}\beta_3$ integrin following treatment with the functionalized liposomes (mean \pm SD, $N = 3$). Significant increase (**** $P < 0.0001$ and *** $P = 0.0001$) in the activated form of the integrin versus the thrombin control was calculated using one-way ANOVA. (D) Scatter dot plot represents the number of platelets expressing P-selectin on the platelet surface after treatment with the functionalized liposomes (mean \pm SD, $N = 3$). Significant change (**** $P < 0.0001$) in the P-selectin expression was calculated using one-way ANOVA. (E) Histogram shows the surface expression of P-selectin in isolated platelets after treatment with the control, vWF-TRAIL liposomes or thrombin. (F) Scatter dot plot represents the number of platelet fragments detectable after exposure to the functionalized liposomes. Significant change (**** $P < 0.0001$ and *** $P = 0.0001$) in the number of platelet fragments was computed using one-way ANOVA. (G) Flow cytometry forward and side scatter plot shows the increase in the number of platelet microparticles in isolated platelets treated with the vWF-TRAIL liposomes or thrombin.



B). Additionally, no effect on integrin activation was observed with functionalized liposomes in comparison to thrombin treatment (Fig. 4C). Likewise, no significant increase in surface P-selectin levels was found in samples treated with functionalized liposomes compared to thrombin (Fig. 4D and E). With regards to the presence of platelet microparticles, no significant increase in the amount of platelet fragments was observed when the platelets were treated with the functionalized liposomes (Fig. 4F and G). These results show that the contact between functionalized liposomes and platelets does not appear to affect the physiological function of platelets. Thus, our results support the use of functionalized liposomes to modify platelets *in situ* as a potential approach to deliver therapeutic drugs to cancer cells effectively with minimal side effects.

TRAIL delivery *via* platelets efficiently kills primary CTCs in the blood of cancer patients with metastatic tumors

In the final part of this study, we examined the efficacy of this approach to kill CTCs in flowing blood collected from cancer patients with metastatic disease. To validate the liposomal therapy as a potential treatment for metastatic disease, blood samples from 10 patients with different types of epithelial tumors were treated with the vWF-TRAIL or naked control liposomes for 4 h under physiological shear conditions (Table 2). First, the platelet adhesion to primary CTCs collected from the cancer patients was evaluated using immunofluorescence microscopy (Fig. 5A). In treated CTCs in flowing blood, we observed that vWF-TRAIL liposomes killed ~60% of CTCs compared to control liposomes (Fig. 5B and C). This TRAIL delivery *via* platelets efficiently killed CTCs from colorectal, prostate, breast and pancreatic cancer patients. The effect of the platelet-mediated TRAIL delivery was less pronounced but still detectable in samples from lung and esophageal cancer patient (Fig. 5D). In summary, TRAIL-coated platelets killed significant numbers of CTCs in the blood of cancer patients with metastatic tumors, supporting the applicability of this approach as a CTC-targeting therapeutic agent.

Based on the well-reported interaction between platelets and tumor cells, several researchers have developed CTC-targeted

drug therapy using platelets as the vehicle. Our previous study demonstrated the use of platelet membrane derived vesicles (PMDV) to coat nanoparticles to deliver TRAIL to tumor cells and showed a reduction in lung metastases.¹⁸ We also previously genetically engineered hematopoietic stem and progenitor cells (HSPCs) to produce platelets expressing TRAIL protein in their surface. This approach delivered TRAIL to tumor cells and reduced the number and size of liver metastases with an additional advantage of avoiding the continuous administration of the therapeutic drug.¹⁹

While these approaches have shown good efficacy by reducing the formation of metastases *in vivo*, some issues persist that should be addressed for translation of platelet based anti-metastatic therapeutic approaches in clinics. Several issues that previous studies present include: (1) the isolation and manipulation of platelets and HSPC is required for the preparation of the therapy, (2) HSPC transplantation to administer the anti-cancer drug, (3) the body irradiation required during the HSPC transplantation to avoid the rejection response in the recipient host and (4) potential infection and disease relapse post-transplantation.¹⁹

Here, we proposed a liposomal formulation based on repurposing/modification of over 70% of platelets in flowing blood to present TRAIL on their surface. This approach was capable of rapidly attaching TRAIL to the platelet surface under physiological shear conditions *via* vWF interaction. Our liposomal approach can overcome most of the issues associated with previous platelet-based TRAIL therapies. First, this liposomal therapy does not require the isolation and modification of platelets *ex vivo* due to the specificity and spontaneous binding of vWF to platelets. Second, the administration of this liposomal therapy is by intravenous injection which avoids the adverse effects associated with HSPC transplantation.^{26–28}

Experimental section

Cancer cells exposed to high magnitude of fluid shear stress

Colonic carcinoma (COLO205) and aggressive breast carcinoma (MDA-MB-231) cells were lifted from culture plates and placed

Table 2 Background information of cancer patients participating in the study

| Patient ID | Carcinoma type | Age | Gender | Metastasis location | Chemotherapy treatment |
|------------|-----------------|-----|--------|----------------------|--|
| 173 | Colon | 57 | M | Liver, adrenal | 5-Fluorouracil, oxaliplatin, leucovorin, avastin |
| 174 | Larynx | 46 | M | Glottis | Cisplatin |
| 175 | Ovary | 58 | F | Liver | Soliris |
| 176 | Lung | 67 | F | Liver | Keytruda |
| 177 | Esophageal | 63 | M | Liver | Xeloda, oxaliplatin |
| 178 | Colon | 57 | M | Lung, liver, adrenal | 5-Fluorouracil, oxaliplatin, leucovorin, avastin |
| 191 | Ureter | 86 | M | Liver | Keytruda |
| 193 | Breast | 83 | F | Lung | Ibrance |
| 196 | Prostate | 69 | M | Lymph nodes, bone | Abiraterone |
| 197 | Pancreas | 56 | M | Malignant ascites | Gemcitabine, abraxane |
| 199 | Colon (sigmoid) | 72 | M | Liver | 5-Fluorouracil |



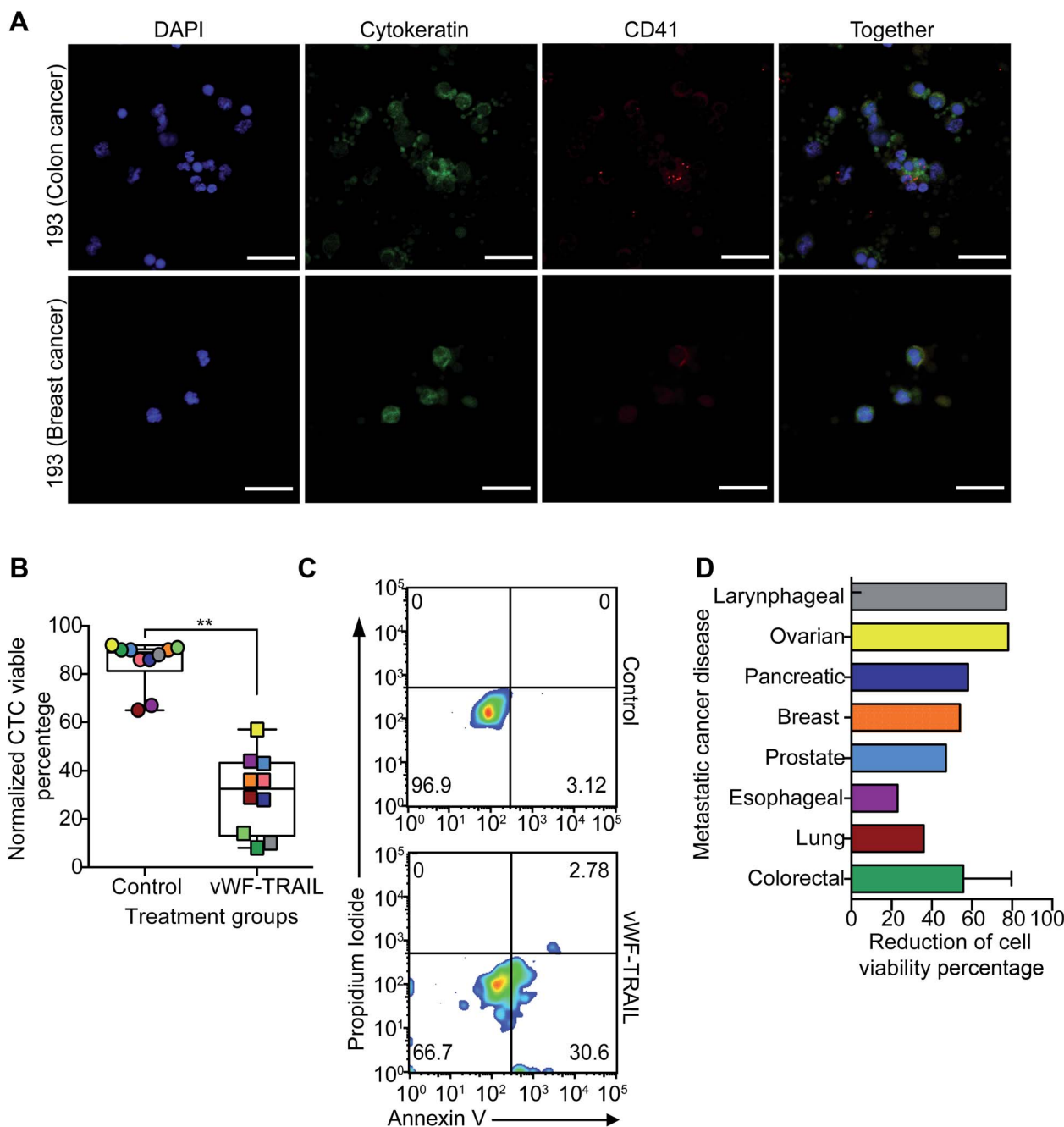


Fig. 5 vWF-TRAIL-liposome bound platelets kill CTCs from the blood of cancer patients with metastatic disease under physiological flow. (A) Immunofluorescence images of platelets and CTCs isolated from the blood of colorectal and breast cancer patients (green is cytochrome, red is CD41, and blue is DAPI). Scale bar is 40 μm . (B) Box and whisker plots show the viability percentage of CTCs treated with naked control and vWF-TRAIL liposomes for 4 h under physiological shear conditions (median \pm range, $N = 20$ from 10 patients). Significance decrease (** $P = 0.0020$) in cell viability was determined using a paired Wilcoxon signed-rank test. (C) Flow cytometry density plots show the viability of CTCs undergoing apoptosis after being treated with the functionalized vWF-TRAIL and naked control liposomes. (D) Bar graph shows the percentage reduction in cell viability for the different cancer types.

in 5 mL syringes with gauge 30 needles (BD) at a concentration of 200 000 cells per mL. Each sample was exposed to 5920 dyn cm^{-2} for 1.08 ms using a syringe pump (Harvard Apparatus, Holliston MA) and were allowed to rest for 2 min between each shear condition to mimic the time it takes a cell to circulate through the body.²³ Isolated human platelets were incubated with the cancer cells for 5 min and then spun down to remove

the unbound platelets. This co-culture of tumor cells and platelets were exposed to high magnitude of shear stress to evaluate the impact of platelets in tumor cell survival under shear stress conditions. Cells were exposed to ten shear pulses. The cells were then plated with regular media overnight. After 24 h, an Annexin V assay was performed to determine the cell viability percentage *via* using flow cytometry.



Preparation of functionalized liposomes

Multilamellar liposomes were prepared using the thin film method, with the following lipids and components: Egg PC, cholesterol, PEG, and maleimide (Avanti) with a weight ratio of 50 : 20 : 1 : 1 (Egg PC : Chol : DSPEG : Maleimide). Corresponding volumes were removed from the stock lipid solutions, mixed in a glass tube and placed in a vacuum chamber overnight. The lipid pellet was resuspended in 1 mL of liposome buffer (HEPES, NaCl pH = 7.4).^{29,30} Multilamellar liposomes were generated using 10 cycles of freeze (2 min), thaw (3 min) and vortex (5 s). Unilamellar liposomes were prepared by 10 extrusion cycles at 55 °C through three different sizes of polycarbonate membranes (400 nm, 200 nm and 100 nm).³⁰ To prepare fluorescently labeled liposomes, the 10% Chol concentration was replaced with green bodipy-labeled cholesterol (Avanti). This basic protocol was previously optimized by our laboratory to produce stable liposomes of final diameter ~150 nm and stable for extended periods. Recombinant human vWF-A₁ domain with (von Willebrand disease type 2B mutation R1306Q) and recombinant human TRAIL were reconstituted with Dulbecco's Phosphate Buffered Saline (DPBS) at 1 mg mL⁻¹ concentration and stored at -80 °C.³¹ The recombinant proteins were thiolated using Trauts reagent (Thermo Fisher) following the manufacturer protocol. Functionalized liposomes were prepared by incubating unilamellar liposomes with 3 µg mL⁻¹ of thiolate vWF-A₁ and TRAIL in the rotator at 4 °C overnight. To determine the efficacy of our novel formulation, four different functionalized liposome groups were prepared: control (no proteins conjugated), vWF (only conjugated with vWF-A₁), TRAIL (only conjugated with TRAIL) and vWF/TRAIL (conjugated with vWF and TRAIL proteins). To confirm the conjugation of proteins on the liposome surface, the liposomes were further characterized by measuring the following parameters: size, surface charge, polydispersity index, concentration of particles, and percentage of particles conjugated using DLS-Malvern Zetasizer and NanoSight NS300. To determine the percentage of particles conjugated with TRAIL protein, vWF-TRAIL conjugated liposomes were incubated with the unconjugated anti-human CD253 (TRAIL) (Clone RIK-2, Biolegend) for overnight in the rotator at 4 °C. Then, using a NanoSight NS300 instrument, the size distribution was evaluated and compared between the vWF-TRAIL conjugate liposomes and these conjugated liposomes incubated with anti-TRAIL. While ELISA is a more commonly used assay of specific protein content, measuring the size shift following antibody incubation provides information on protein content on a per-liposome basis which was desired.

Cytotoxicity of functionalized liposomes

Colonic carcinoma (COLO205) and aggressive breast carcinoma (MDA-MB-231) cell lines were obtained from ATCC and used to determine the cytotoxicity of our therapeutic formulation in benchtop experiments. The cells were cultured in 12-multiwell plates at a density of 200 000 cells per mL for 24 h. The culture medium was replaced with serum-free media and 20 µL of functionalized liposomes were added. We changed to serum-

free media to maintain the number of cells equal between samples. The viability of cells was measured using an Annexin V apoptosis assay (BD) following 24 h of incubation. In this assay, the cells were removed from the culture plates and stained following the manufacturer's protocol. Following this, the viable cell percentage was determined using flow cytometry.

Adhesion of functionalized liposomes to platelets under physiological shear stress

To determine the adhesion of liposomes to human platelets, a cone-and-plate viscometer was used to apply a defined shear stress to the samples. The cup and spindle of the viscometer were blocked with 2 mL of 5% Bovine Serum Albumin (BSA, Sigma) for 30 min. Then, 480 µL of whole blood was incubated with 20 µL of fluorescently-labeled functionalized liposomes in the viscometer for 30 min. The blood was removed from the viscometer using Hank's Balanced Salt Solution (HBSS) buffer and spun down at 200×g for 5 min. The platelet-rich plasma was collected into a fresh centrifuge tube, washed with twice the volume of Tyrodes buffer (Sigma Aldrich), and spun down at 1400×g for 5 min. The platelet pellet was gently resuspended using 480 µL of Tyrodes buffer. Then samples were stained using anti-human CD41 (a platelet marker) conjugated with Alexa Fluor 405 (Clone HIP8, Biolegend) for 20 min. The adhesion of liposomes to the platelets was evaluated using flow cytometry, by measuring the percentage of CD41-labeled platelets that were positive for fluorescently-labeled liposomes.

Cytotoxicity of functionalized liposomes in an ex vivo CTC model

Colo205 and MDA-MB-231 cells were spiked into the blood from healthy human donors (500 µL) and treated with functionalized liposomes in a cone-and-plate viscometer for a period of 2 h. The viscometer was used to mimic CTC dynamics in the bloodstream. Blood samples were collected in citrate-coated tubes from healthy volunteers that had not received any medication within a week. About 200 000 cells were removed from cell culture, stained with 25 µg mL⁻¹ of Cell Tracker 7-amino-4-chloromethylcoumarin (CMAC) for 20 min, washed twice with DPBS, incubated with 450 µL of human blood and placed in a viscometer. The viscometer (cup and spindle) was blocked using 2 mL of 5% BSA solution at room temperature for 30 min before adding the sample. Once the cells were mixed and placed in the viscometer, 50 µL of functionalized liposomes were added to the respective samples and the samples were subjected to shear force of 225 s⁻¹ for 2 h. Afterwards, the blood was removed from the viscometer and washed carefully with 4-times the volume of HBSS (no calcium and magnesium). The blood samples were layered over 2-times the volume of ficoll and spun down at 2000×g for 15 min with no brake to isolate the cancer cells. Then, the buffy coat was isolated and washed using twice the volume of HBSS buffer and spun down at 300×g for 10 min. The cell pellet was resuspended in media and cultured overnight. Then, the cells were removed from culture and stained with annexin V, propidium iodide and 10 µg mL⁻¹ of anti-human CD41 conjugated with Alexa Fluor 647 for 15 min



following the manufacturer's protocol. Cell viability was determined by measuring the number of unlabeled cells (negative for annexin V and propidium iodide) using a flow cytometer (Cell Tracker labeled events). To evaluate the adhesion of platelets to tumor cells we evaluated the positive CD41 events in the Cell Tracker labeled events using the proper isotype control.

Intracellular calcium content

Peripheral blood was collected in a citrate coated tubes and the platelets were isolated as we mentioned before in the materials and method section. The isolated platelets were stained with 100 μL of 3.34 $\mu\text{g mL}^{-1}$ of Fluo-4 and 6.67 $\mu\text{g mL}^{-1}$ of Fura Red for 20 min. Then, 100 μL of isolated platelets were incubated with 10 μL of conjugated liposomes for 15 min. At the end of the incubation, 200 μL of DPBS were added to the samples and the ratio of cytosolic calcium concentration was evaluated using flow cytometry. As a positive control, the platelets were treated with 1 U mL^{-1} of thrombin.

Activation of platelets by conjugated liposomes

Peripheral blood was collected in citrate coated tubes and platelets were isolated as described above. Around 100 μL of platelets were incubated for 15 min with 10 μL of the conjugated liposomes. Then the samples were fixed using 100 μL of 4% paraformaldehyde for 15 min. The samples were washed and stained using 100 μL of 10 $\mu\text{g mL}^{-1}$ of annexin V conjugated with Biotin (Biolegend) for 30 min. After, the samples were treated with 100 μL of 10 $\mu\text{g mL}^{-1}$ of streptavidin conjugated with Alexa Fluor 594, 10 $\mu\text{g mL}^{-1}$ of anti-human CD41 conjugated with Alexa Fluor 647 (Clone HI30, Biolegend), 10 $\mu\text{g mL}^{-1}$ of anti-human CD41/CD61 (Clone PAC-1, Biolegend) and 10 $\mu\text{g mL}^{-1}$ of anti-human CD61P (Clone AK-4, Biolegend) for 30 min. The presence of activated integrin, exposure of P-selectin and the formation of platelet fragments were identified by the positive staining of these antibodies with respect to their respective isotypes using flow cytometry. As a positive control a 5 U mL^{-1} dose of thrombin was administered to some cells.

Efficacy of functionalized liposomes in killing CTCs from metastatic cancer patients

Peripheral blood was collected from cancer patients diagnosed with metastatic carcinoma that had already underwent chemotherapy as the first line of treatment, after informed consent (Guthrie Clinic IRB # 1808-45). All experiments were performed in accordance with the U.S. Federal Policy for the Protection of Human Subjects, and approved by the Institutional Review Board of the Guthrie Clinic. Study participants were fully informed regarding the purposes of the study and consent was obtained.

Blood samples from 10 patients with metastatic tumors were collected and used in this study. The blood samples were collected at the Guthrie Clinical Research Center and shipped to Vanderbilt University overnight. About 2 mL of blood was incubated with 100 μL of functionalized liposomes and placed in the viscometer for 4 h at 120 s^{-1} . The blood samples were removed from the viscometer and the buffy coat layer was

isolated as described above. The buffy coat was incubated with anti-human CD45 magnetic beads for 15 min, following the manufacturer's protocol (Mylteni Biotech) and placed in a column within a magnetic field. The column was washed three times and the eluted fraction of cells contained CTCs. These treated CTCs were cultured overnight.³² The following day, CTCs were removed from culture, stained with propidium iodide for 15 min and fixed with 4% paraformaldehyde (Electron Microscopy Sciences). The CTC suspensions were cytospun on microscopic slides, permeabilized using 100 μL of 0.25% triton (Fisher Scientific) for 15 min and further blocked with 5% BSA and 5% goat serum (Thermo Fisher) for 1 h. Cells were stained using a two-step immunostaining process (30 min each) using: (i) 10 $\mu\text{g mL}^{-1}$ of anti-human CD45 conjugated with biotin (Clone HI30, Biolegend) and (ii) 10 $\mu\text{g mL}^{-1}$ of streptavidin conjugated with Alexa Fluor 594 (Biolegend) and 10 $\mu\text{g mL}^{-1}$ of anti-cytokeratin conjugated with FITC (Clone CAM 5.2, BD). The cells were washed three times after each staining using 200 μL of DPBS with 0.02% Tween (Research Products). Finally, 15 μL of mounting media with 4',6-diamidino-2-phenylindole (DAPI) was added to the slide, covered with a coverslip and sealed using nail polish. The slides were imaged using a Zeiss LSM 710 confocal microscope. The CTCs were identified and enumerated as viable cells using the following criteria: (i) positive for cytokeratin, (ii) negative for CD45, (iii) positive for the nuclear stain DAPI and (iv) negative for necrotic stain propidium iodide. The cells were counted using Image J software.

Statistical analysis

To analyze the flow cytometry data, FlowJo software was used. All of the statistical analyses were carried out using Graph Pad (PRISM 6.0) for Mac OS X. All of the statistical tests were treated as two-sided and calculated at level of significance $\alpha = 0.05$. Paired *t* and ANOVA tests were used to compare two groups and more than two groups, respectively. Two-way ANOVA test was used to compare two groups in two different factors. For ANOVA test that included multiple comparison, Turkey adjustments were applied and the adjusted *P* value used.

Conclusion

A strong relationship between thrombosis and cancer metastasis has been elucidated in the literature.³³⁻³⁵ During metastasis, platelets play an important role in promoting tumor cell growth, invasion, survival in the circulation, extravasation and the overgrowth of these existing cells in distant organs.⁸ Here, we demonstrated the use of a liposomal therapy as a straightforward approach to repurpose platelets *in situ* to effectively target and kill CTCs in the bloodstream while minimizing any cytotoxic effects to normal tissues. Despite these promising results, questions remain related to the efficacy of this platelet-based therapy to prevent cancer metastasis using clinically relevant *in vivo* models. Further studies using surgical tumor resection murine models of different cancer types are needed to take advantage of the hemostatic activity of the platelet carriers. These studies could demonstrate the delivery of therapeutic



agent systemically to target metastasis and to prevent cancer recurrence.²⁰ The platelet-liposomal therapy is a promising approach that could be used in combination with surgery to prevent cancer recurrence and cancer metastasis in patients.

Author contributions

N. O. O designed and performed the experiments, analyzed research data, and wrote the manuscript. J. R. M. developed CTC analysis protocols and B. L. provided the clinical samples. M. R. K conceived of the study and edited the manuscript.

Conflicts of interest

The authors have no conflicts of interest to disclose.

Acknowledgements

We thank all of the volunteers who participated in this study. We also thank Tejas Subramanian and Antonio Glenn for their contributions to the study. We thank Nidhi Jyotsana for reviewing the manuscript.

References

- 1 J. Li and M. R. King, Adhesion Receptors as Therapeutic Targets for Circulating Tumor Cells, *Frontiers in Oncology*, 2012, **2**(79), 1–9, DOI: 10.3389/fonc.2012.00079.
- 2 A. W. Lambert, D. R. Pattabiraman and R. A. Weinberg, Emerging Biological Principles of Metastasis, *Cell*, 2017, **168**(4), 670–691, DOI: 10.1016/j.cell.2016.11.037.
- 3 D. F. Quail and J. A. Joyce, Microenvironmental Regulation of Tumor Progression and Metastasis, *Nat. Med.*, 2013, **19**(11), 1423–1437, DOI: 10.1038/nm.3394.
- 4 M. R. Junttila and F. J. de Sauvage, Influence of Tumour Micro-Environment Heterogeneity on Therapeutic Response, *Nature*, 2013, **501**(7467), 346–354, DOI: 10.1038/nature12626.
- 5 D. Hanahan and L. M. Coussens, Accessories to the Crime: Functions of Cells Recruited to the Tumor Microenvironment, *Cancer Cell*, 2012, **21**(3), 309–322, DOI: 10.1016/j.ccr.2012.02.022.
- 6 V. Ganapathy, P. V. Moghe and C. M. Roth, Targeting Tumor Metastases: Drug Delivery Mechanisms and Technologies, *J. Controlled Release*, 2015, **219**, 215–223, DOI: 10.1016/j.jconrel.2015.09.042.
- 7 J. Li, C. C. Sharkey, D. Huang and M. R. King, Nanobiotechnology for the Therapeutic Targeting of Cancer Cells in Blood, *Cell. Mol. Bioeng.*, 2015, **8**(1), 137–150, DOI: 10.1007/s12195-015-0381-z.
- 8 N. Ortiz-Otero, Z. Mohamed and M. R. King, Platelet-Based Drug Delivery for Cancer Applications, in *Biomechanics in Oncology*, ed. C. Dong, N. Zahir and K. Konstantopoulos, Springer International Publishing, Cham, 2018, vol. 1092, pp. 235–251, DOI: 10.1007/978-3-319-95294-9_12.
- 9 O. J. T. McCarty, S. Jadhav, M. M. Burdick, W. R. Bell and K. Konstantopoulos, Fluid Shear Regulates the Kinetics and Molecular Mechanisms of Activation-Dependent Platelet Binding to Colon Carcinoma Cells, *Biophys. J.*, 2002, **83**(2), 836–848, DOI: 10.1016/S0006-3495(02)75212-0.
- 10 B. Nieswandt, M. Hafner, B. Echtenacher and D. N. Männel, Lysis of Tumor Cells by Natural Killer Cells in Mice Is Impeded by Platelets, *Cancer Res.*, 1999, **59**(6), 1295–1300.
- 11 L. J. Gay and B. Felding-Habermann, Contribution of Platelets to Tumour Metastasis, *Nat. Rev.*, 2011, **11**, 123–134.
- 12 Y. Yu, X. D. Zhou, Y. K. Liu, N. Ren, J. Chen and Y. Zhao, Platelets Promote the Adhesion of Human Hepatoma Cells with a Highly Metastatic Potential to Extracellular Matrix Protein: Involvement of Platelet P-Selectin and GP IIb-IIIa, *J. Cancer Res. Clin. Oncol.*, 2002, **128**(5), 283–287, DOI: 10.1007/s00432-002-0325-6.
- 13 J. L. Stevenson, A. Varki and L. Borsig, Heparin Attenuates Metastasis Mainly Due to Inhibition of P- and L-Selectin, but Non-Anticoagulant Heparins Can Have Additional Effects, *Thromb. Res.*, 2007, **120**, S107–S111, DOI: 10.1016/s0049-3848(07)70138-x.
- 14 T. M. H. Niers, C. P. W. Klerk, M. DiNisio, C. J. F. Van Noorden, H. R. Büller, P. H. Reitsma and D. J. Richel, Mechanisms of Heparin Induced Anti-Cancer Activity in Experimental Cancer Models, *Critical Reviews in Oncology/Hematology*, 2007, **61**(3), 195–207, DOI: 10.1016/j.critrevonc.2006.07.007.
- 15 P. Xu, H. Zuo, B. Chen, R. Wang, A. Ahmed, Y. Hu and J. Ouyang, Doxorubicin-Loaded Platelets as a Smart Drug Delivery System: An Improved Therapy for Lymphoma, *Sci. Rep.*, 2017, **7**(1), 42632, DOI: 10.1038/srep42632.
- 16 H. Ye, K. Wang, M. Wang, R. Liu, H. Song, N. Li, Q. Lu, W. Zhang, Y. Du, W. Yang, L. Zhong, Y. Wang, B. Yu, H. Wang, Q. Kan, H. Zhang, Y. Wang, Z. He and J. Sun, Bioinspired Nanoplatelets for Chemo-Photothermal Therapy of Breast Cancer Metastasis Inhibition, *Biomaterials*, 2019, **206**, 1–12, DOI: 10.1016/j.biomaterials.2019.03.024.
- 17 P. Xu, H. Zuo, R. Zhou, F. Wang, X. Liu, J. Ouyang and B. Chen, Doxorubicin-Loaded Platelets Conjugated with Anti-CD22 MAbs: A Novel Targeted Delivery System for Lymphoma Treatment with Cardiopulmonary Avoidance, *Oncotarget*, 2017, **8**(35), 58322–58337, DOI: 10.18632/oncotarget.16871.
- 18 J. Li, Y. Ai, L. Wang, P. Bu, C. C. Sharkey, Q. Wu, B. Wun, S. Roy, X. Shen and M. R. King, Targeted Drug Delivery to Circulating Tumor Cells via Platelet Membrane-Functionalized Particles, *Biomaterials*, 2016, **76**, 52–65, DOI: 10.1016/j.biomaterials.2015.10.046.
- 19 J. Li, C. C. Sharkey, B. Wun, J. L. Liesveld and M. R. King, Genetic Engineering of Platelets to Neutralize Circulating Tumor Cells, *J. Controlled Release*, 2016, **228**, 38–47, DOI: 10.1016/j.jconrel.2016.02.036.
- 20 X. Zhang, J. Wang, Z. Chen, Q. Hu, C. Wang, J. Yan, G. Dotti, P. Huang and Z. Gu, Engineering PD-1-Presenting Platelets for Cancer Immunotherapy, *Nano Lett.*, 2018, **18**(9), 5716–5725, DOI: 10.1021/acs.nanolett.8b02321.



- 21 A. J. Gareau, C. Brien, S. Gebremeskel, R. S. Liwski, B. Johnston and M. Bezuhly, Ticagrelor Inhibits Platelet-Tumor Cell Interactions and Metastasis in Human and Murine Breast Cancer, *Clin. Exp. Metastasis*, 2018, **35**(1–2), 25–35, DOI: 10.1007/s10585-018-9874-1.
- 22 A.-L. Papa, A. Jiang, N. Korin, M. B. Chen, E. T. Langan, A. Waterhouse, E. Nash, J. Caroff, A. Graveline, A. Vernet, A. Mammoto, T. Mammoto, A. Jain, R. D. Kamm, M. J. Gounis and D. E. Ingber, Platelet Decoys Inhibit Thrombosis and Prevent Metastatic Tumor Formation in Preclinical Models, *Sci. Transl. Med.*, 2019, **11**(479), eaau5898, DOI: 10.1126/scitranslmed.aau5898.
- 23 J. M. Barnes, J. T. Nauseef and M. D. Henry, Resistance to Fluid Shear Stress Is a Conserved Biophysical Property of Malignant Cells, *PLoS One*, 2012, **7**(12), e50973, DOI: 10.1371/journal.pone.0050973.
- 24 M. J. Mitchell, C. Denais, M. F. Chan, Z. Wang, J. Lammerding and M. R. King, Lamin A/C Deficiency Reduces Circulating Tumor Cell Resistance to Fluid Shear Stress, *Am. J. Physiol.: Cell Physiol.*, 2015, **309**(11), C736–C746, DOI: 10.1152/ajpcell.00050.2015.
- 25 M. J. Mitchell, E. Wayne, K. Rana, C. B. Schaffer and M. R. King, TRAIL-Coated Leukocytes That Kill Cancer Cells in the Circulation, *Proc. Natl. Acad. Sci. U. S. A.*, 2014, **111**(3), 930–935, DOI: 10.1073/pnas.1316312111.
- 26 A. Paix, D. Antoni, W. Waissi, M.-P. Ledoux, K. Bilger, L. Fornecker and G. Noel, Total Body Irradiation in Allogeneic Bone Marrow Transplantation Conditioning Regimens: A Review, *Critical Reviews in Oncology/Hematology*, 2018, **123**, 138–148, DOI: 10.1016/j.critrevonc.2018.01.011.
- 27 M. Tuthill, Hatzimichael. Hematopoietic Stem Cell Transplantation, *Stem Cells Cloning: Adv. Appl.*, 2010, **105**, DOI: 10.2147/sccaa.s6815.
- 28 Y. Inamoto, N. N. Shah, B. N. Savani, B. E. Shaw, A. A. Abraham, I. A. Ahmed, G. Akpek, Y. Atsuta, K. S. Baker, G. W. Basak, M. Bitan, Z. DeFilipp, T. K. Gregory, H. T. Greinix, M. Hamadani, B. K. Hamilton, R. J. Hayashi, D. A. Jacobsohn, R. T. Kamble, K. A. Kasow, N. Khera, H. M. Lazarus, A. K. Malone, M. T. Lupo-Stanghellini, S. P. Margossian, L. S. Muffly, M. Norkin, M. Ramanathan, N. Salooja, H. Schoemans, J. R. Wingard, B. Wirk, W. A. Wood, A. Yong, C. N. Duncan, M. E. D. Flowers and N. S. Majhail, Secondary Solid Cancer Screening Following Hematopoietic Cell Transplantation, *Bone Marrow Transplant.*, 2015, **50**(8), 1013–1023, DOI: 10.1038/bmt.2015.63.
- 29 S. Chandrasekaran, M. J. McGuire and M. R. King, Sweeping Lymph Node Micrometastases off Their Feet: An Engineered Model to Evaluate Natural Killer Cell Mediated Therapeutic Intervention of Circulating Tumor Cells That Disseminate to the Lymph Nodes, *Lab Chip*, 2014, **14**(1), 118–127, DOI: 10.1039/c3lc50584g.
- 30 S. Chandrasekaran, M. F. Chan, J. Li and M. R. King, Super Natural Killer Cells That Target Metastases in the Tumor Draining Lymph Nodes, *Biomaterials*, 2016, **77**, 66–76, DOI: 10.1016/j.biomaterials.2015.11.001.
- 31 E. Fressinaud, C. Mazurier and D. Meyer, Molecular Genetics of Type 2 von Willebrand Disease, *Int. J. Hematol.*, 2002, **75**(1), 9–18.
- 32 A. Meye, U. Bilkenroth, U. Schmidt, S. Füssel, K. Robel, A. M. Melchior, K. Blümke, D. Pinkert, F. Bartel, C. Linne, H. Taubert and M. P. Wirth, Isolation and Enrichment of Urologic Tumor Cells in Blood Samples by a Semi-Automated CD45 Depletion AutoMACS Protocol, *Int. J. Oncol.*, 2002, **21**(3), 521–530.
- 33 B. Pulluri, B. Littenberg, I. Lal, C. E. Holmes and S. Ades, Risk Factors for Venous Thromboembolism in Metastatic Colon Cancer Patients in the Contemporary Treatment Era: A SEER-Medicare Data Analysis, *Blood*, 2016, **128**(22), 2598.
- 34 U. T. Khan, A. J. Walker, S. Baig, T. R. Card, C. C. Kirwan and M. J. Grange, Venous Thromboembolism and Mortality in Breast Cancer: Cohort Study with Systematic Review and Meta-Analysis, *BMC Cancer*, 2017, **17**(1), 747, DOI: 10.1186/s12885-017-3719-1.
- 35 N. Abdol Razak, G. Jones, M. Bhandari, M. Berndt and P. Metharom, Cancer-Associated Thrombosis: An Overview of Mechanisms, Risk Factors, and Treatment, *Cancers*, 2018, **10**(10), 380, DOI: 10.3390/cancers10100380.

